OPEN ACCESS
IOP Publishing
Journal of Physics B: Atomic, Molecular and Optical Physics
J. Phys. B: At. Mol. Opt. Phys. **54** (2021) 114001 (8pp)
https://doi.org/10.1088/1361-6455/abfe00

Strong-field triple ionisation of atoms with p^3 valence shell

Jakub S Prauzner-Bechcicki[1,*], Dmitry K Efimov[2,3], Michał Mandrysz[2] and Jakub Zakrzewski[2,4]

[1] Instytut Fizyki imienia Mariana Smoluchowskiego, Jagiellonian University in Krakow, Łojasiewicza 11, 30-348 Kraków, Poland
[2] Institute of Theoretical Physics, Jagiellonian University in Krakow, Łojasiewicza 11, 30-348 Kraków, Poland
[3] Department of Theoretical Physics, Faculty of Fundamental Problems of Technology, Wrocław University of Science and Technology, 50-370 Wrocław, Poland
[4] Mark Kac Complex Systems Research Center, Jagiellonian University in Krakow, Łojasiewicza 11, 30-348 Kraków, Poland

E-mail: jakub.prauzner-bechcicki@uj.edu.pl

Received 17 February 2021, revised 7 April 2021
Accepted for publication 4 May 2021
Published 9 June 2021

Abstract

The interaction of strong pulsed femtosecond laser field with atoms having three equivalent electrons in the outer shell (p^3 configuration, e.g. nitrogen) is studied via numerical integration of a time-dependent Schrödinger equation on a spatial grid. Single ionisation, double ionisation (DI) and triple ionisation (TI) yields originating from a completely antisymmetric wave function are calculated and extracted using a restricted-geometry model with the soft-core potential and three active electrons. The observed suppression of the ionisation yields for the non-sequential processes, in both DI and TI cases, is attributed to the action of the Pauli principle. Compared against earlier results investigating the s^2p^1 configuration, we propose that the differences found here might in fact be accessible through electron's momentum distribution.

Keywords: non-sequential ionization, strong pulsed laser fields, *ab initio* calculations, restricted-geometry model, triple ionization, wave function symmetry

(Some figures may appear in colour only in the online journal)

1. Introduction

The study of correlations is the study of the complexity of the world around us. One of the amazing manifestations of the existence of correlations in nature is the phenomenon of non-sequential double ionisation (NSDI) in strong laser fields [1, 2]. Reports from experiments showing the recorded double ionisation (DI) yield higher by several orders of magnitude than expected in the sequential electron escape processes [3–5], followed by the measurements of the ion recoil momentum and latter extraction of electrons' momenta distributions with the famous finger-like structure [6, 7] forced researchers to acknowledge the fundamental role of electron–electron correlations played in NSDI. Along with the experimental work, there were attempts to theoretically explain the observed phenomenon. It is now recognized that the process has a stepwise character and the rescattering is an important ingredient [8]. In the process one of the electrons tunnels and begins to move away from its parent ion. When the phase of the field changes (we deal with short pulses, usually having the wavelength on the border of visible and infrared light), the electron is turned back, accelerated and recollides with the ion. As a result of the recollision, energy transfer occurs and consequently the escape of the second electron is allowed.

* Author to whom any correspondence should be addressed.

Research on very intense laser pulses leading to multiple ionisation began in the 1980s [9–14]. These studies resulted in discussions about the sequential or collective character of electron emission [10, 15–23]; with the subsequent detailed understanding of rescattering it turned out that the non-sequential events for two active electrons are most important at *intermediate* laser intensities [3–5]. Similarly if rescattering events affect strongly ionisation process involving three or more electrons, then we speak of non-sequential multiple ionisation [24]. However, theoretical analysis of events involving more than two electrons is very difficult. This is evidenced by the fact that full-size, i.e. taking into account all spatial dimensions for each electron, quantum calculations even for two electrons are still very rare [25–29]. Simplified quantum models with a reduced number of dimensions are often used to overcome the numerical difficulty [6, 30–40]. And in the case when three and more electrons are involved, classical or semi-classical calculations are often used [41–47] with the independent electron model [20] likely being applicable only at very high intensities. On the other hand experimental progress in the area is quite spectacular [48–51].

We have recently shown that it is possible to construct a model with a reduced geometry that enables a study of triple ionisation (TI) [36]. Importantly, the electronic configuration of the target atoms begins to play a significant role. In the case when two electrons are involved in the process, it is usually assumed that they have opposite spins and therefore the spatial part of the wave function is symmetrical. When three active electrons are involved the spatial part of the wave function cannot be symmetric. The electron configuration of the target atoms is reflected in the symmetry of the wave function under consideration. And so, for alkali metals with s^2p^1 configurations we will have a spatial wave function which is partially antisymmetric, while for elements with p^3 configuration (e.g. nitrogen) we will have a completely antisymmetric function. The difference between these two possible situations and its possible impact on the ionisation dynamics has not been fully explored up till now. Importantly, due to symmetry properties of the ground state for atoms with the s^2p^1 configuration it is not possible to reduce the problem of DI (occurring in the three electron model) to the model of two active electrons [38]. In contrary, such a reduction is possible in the case of atoms with the p^3 configuration [40].

TI dynamics is supposed to depend on the initial spin symmetry as well. In the previous work [36] we considered TI events in atoms with the s^2p^1 configuration. In that case (ground state energy -4.63 a.u.), the dominant TI channel was the sequential escape for fields with amplitudes $F = 0.2$ and higher (in the following we use atomic units, unless otherwise stated). Channels associated with the non-sequential escape, i.e. (i) three electrons being ejected simultaneously, (ii) first a single then two electrons are ionised, and (iii) first two and then one electron are ejected, are important for fields with amplitudes less than $F = 0.2$. For the range of the analysed field amplitudes, the process in which one electron is ionised first, and then two, plays a dominant role among the three mentioned paths of non-sequential escape.

In the present paper, we concentrate on the influence of the initial state symmetry on TI. For this purpose, we analyse TI events for atoms with the p^3 configuration in the outer shell and compare the results with the physics in the s^2p^1 configuration. The crucial question we try to answer is to what extent the symmetry of the initial wavefunction affects the dynamics of the ionisation process, notably sequential and non-sequential events. As far as we know this problem has not been addressed before. Note, however, using species with different initial configuration, i.e. s^2p^1 and p^3, as a starting point inevitably necessitates models with different sets of ionisation potentials thus comparing of the absolute values of ionisation yields is pointless. Still, the overall shape of ionisation yields as functions of the field amplitude or the relative impact of various ionisation channels may be safely juxtaposed.

The paper is structured as follows. Section 2.1 describes the model we analyse and in particular the dimensional reduction applied. Section 2.2 presents the space-division approach that allows us to calculate contributions of different ionisation channels to (multi)-electron ionisation. In section 3 we present the main results and compare them to the results obtained in our previous work [40] for a different electron configuration. We conclude in section 4.

2. Model and methods

2.1. Model

Due to the computational complexity it is virtually impossible nowadays to tackle the three electron problem numerically in the full configuration space. Therefore, we employ a judiciously designed restricted-space model [36, 42] in which each of the three electrons is allowed to move along one-dimensional (1D) track. The chosen 1D-tracks are equivalent to the lines along which the saddles, formed by the instantaneous electric field in the potential, move when the field amplitude is varied (see figure 1(a)). The saddles and their motion were determined with the application of local stability analysis in the adiabatic potential [42, 52, 53]. The Hamiltonian in the restricted-space reads (in atomic units):

$$H = \sum_{i=1}^{3} \frac{p_i^2}{2} + V_{\mathrm{a}} + V_{\mathrm{int}}, \tag{1}$$

where V_{a} is the atomic potential:

$$V_{\mathrm{a}} = -\sum_{i=1}^{3} \frac{3}{\sqrt{r_i^2 + \epsilon^2}} + \sum_{i,j=1;i<j}^{3} \frac{q_{\mathrm{ee}}^2}{\sqrt{(r_i - r_j)^2 + r_i r_j + \epsilon^2}}, \tag{2}$$

reproducing the experimental single-ionisation (SI) and DI potentials for a nitrogen atom with soft-core parameter $\epsilon = \sqrt{1.02}$ and effective electron–electron charges $q_{\mathrm{ee}} = \sqrt{0.5}$ (same as in [40]). Potential V_{int} describes an interaction with the external field:

$$V_{\mathrm{int}} = \sqrt{\frac{2}{3}} F(t)(r_1 + r_2 + r_3). \tag{3}$$

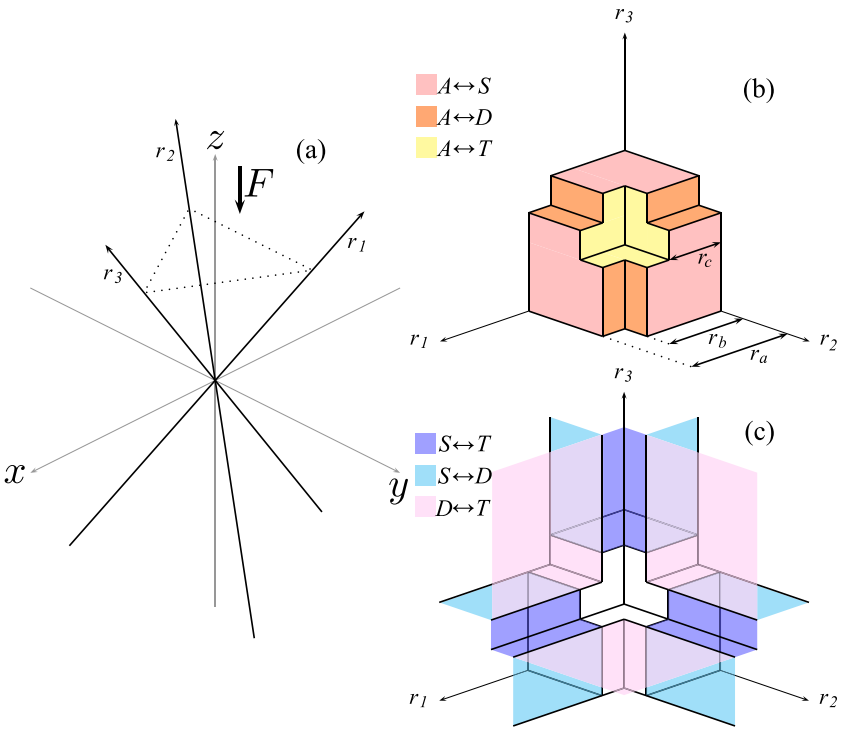

Figure 1. The restricted-space model [40]. Panel (a): the geometry of the model with respect to three-dimensional space: electrons propagate along r_1, r_2, and r_3 axes. The field polarization direction, $\vec{F}$, is indicated by the arrow. Panels (b) and (c)—visualization of the space division within the model as used for calculation of probability fluxes. The space is divided into regions corresponding to neutral states (A), singly ionised states (S), doubly ionised states (D), and triply ionised states (T). The borders between respective regions are marked with different colours as shown in each panel: on panel (b) borders A–S, A–D and A–T are depicted, whereas on panel (c) borders S–D, S–T and D–T. The border distances are $r_a = 12.5$ a.u., $r_b = 7$ a.u., and $r_c = 5$ a.u., respectively.

r_i and p_i are the i'th electron's coordinate and conjugated momentum, respectively. The field is defined via its vector potential, $F(t) = -\partial A/\partial t$, and is polarized along the z axis in full space:

$$A(t) = \frac{F_0}{\omega_0}\sin^2\left(\frac{\pi t}{T_\mathrm{p}}\right)\sin(\omega_0 t + \varphi), \quad 0 < t < T_\mathrm{p}. \tag{4}$$

Here F_0, ω_0, $T_0 = 2\pi n_\mathrm{c}/\omega_0$, φ and n_c are the field amplitude, the pulse frequency, the pulse length, the carrier–envelope phase and the number of cycles. In the following we set $\omega_0 = 0.06$ which corresponds to 760 nm of laser wavelength and the number of cycles, $n_\mathrm{c} = 5$. The field amplitude and the carrier–envelope phase may be varied. We have found numerically that the reported dynamics is only weakly dependent on the carrier–envelope phase hence the results for $\varphi = 0$ are presented only. As the field is polarized along the z axis in the full space it has to be projected onto r_i tracks. The projection imposes the geometric factor $\sqrt{2/3}$ in (3).

2.2. Methods

The time-dependent Schrödinger equation for the above Hamiltonian is solved on a homogeneously spaced grid in three dimensions by a standard split-operator technique supplemented with FFT [36]. While the method is a straightforward generalization of our previous two-electron code [32] to three dimensions the choice of the symmetry of the initial state plays an important role. The standard approach for two electron is to assume a spatially symmetric (with respect to exchange of electrons) wavefunction. That implies that electrons are assumed in a singlet spin state. For three electrons there are two possibilities. Either all the electrons have spin projection in the same direction as in p^3 configuration, e.g., ground state of nitrogen, or only two electrons have the same orientation of spin with the remaining one having the opposite orientation (like in s^2p^1 configuration). The symmetry of the initial state is preserved in the time evolution. The latter, Li-like case [54] was considered by us in [36], while a comparison between two and three active electrons for p^3 configuration has been performed in [40]. Nowhere, however, a real comparison between both three active electron models have been done. This is the aim of the present work where also, for the first time, three electron ionisation for p^3 electrons is analysed in detail.

To find the initial wavefunction for p^3 we use imaginary time propagation scheme (in the absence of the laser pulse) in the subspace of totally antisymmetric wavefunctions under the $r_i \leftrightarrow -r_i$ exchange as well as $r_i \leftrightarrow r_j$. The real time propagation is efficiently parallelised. The largest grid sizes required about 9 days of calculations on 96 cores.

To calculate ionisation yields we apply a space division method introduced in the seminal work treating DI of He [55]. This approach was commonly used in both classical and quantum-mechanical calculations [36, 37, 54, 55]—compare figures 1(b) and (c). The full configuration space of the problem is divided into non-overlapping regions which fully

cover the space. A very simplistic approach assumes that if the distance of ith electron from the nucleus exceeds a given threshold value, this electron is ionised. Such an approach was used for TI of Li [54] but this approach does not allow to distinguish easily sequential and non-sequential processes. Our approach [36, 37] is a straightforward generalisation of two electron technique [55] to the slightly more complicated three electron case. The total configuration space is divided symmetrically into regions corresponding to neutrals (A), singly ionised species (S), doubly ionised atoms (D) and triply ionised ones (T) using three characteristic length scales (radii) r_a, r_b, r_c with $r_a > r_b > r_c$. For the sake of simplicity, we describe only the case $0 < r_1 < r_2 < r_3$, leaving out the other possible permutations. If all $r_i < r_c$ then the atom remains intact, if all $r_i > r_c$ the system is triply ionised (region T). If $r_2 < r_b$ (thus also r_1) but $r_3 > r_a$ it belongs to the region S (single ionised species). Finally, if $r_1 < r_c$, $r_2 > r_b$ and $r_3 > r_b$ the system is doubly ionised—region D. Taking all possible permutations of r_i into account this approach splits the full configuration space between distinct regions associated with the neutral atom (A), singly (S), doubly (D), and triply (T) ionised species. The populations of A, S, D and T regions are calculated as integrated probability fluxes through the borders of the respective regions. The particular values for the radii of the borders r_a, r_b, r_c are to a certain degree arbitrary and their choice affects quantitatively the results. However, as verified before [36–38, 40, 55] the chosen values provide results that reflect the correct trends in the dynamics of the studied systems. Further on we assume $r_a = 12$ a.u., $r_b = 7$ a.u., and $r_c = 5$ a.u. following the choice made for two electron case in [55] as well as for three electrons [36, 38, 40].

A much simpler case of two-electron system is described in detail in [32, 37], here we just briefly mention the methodology behind the calculations and present the borders A–S, A–D, and A–T in figure 1(b) and borders S–D, S–T, and D–T figure 1(c). The instantaneous value of the population in region R is calculated via the integral:

$$P_R(\mathbf{r}, t) = P_R(\mathbf{r}, 0) - \int_0^t f_R(\tau)\mathrm{d}\tau, \tag{5}$$

where $f_R(\tau)$ represents probability flux over border of the R region, i.e.

$$f_R(\tau) = -\iint_{\partial R} \mathbf{j}(\mathbf{r}, \tau) \cdot \mathrm{d}\boldsymbol{\sigma}. \tag{6}$$

Here $\mathbf{j}(\mathbf{r}, \tau)$ is the standard quantum-mechanical current, $\mathrm{d}\boldsymbol{\sigma}$ is a surface element and ∂R symbolizes border of the region R.

The space-division method allows straightforwardly to distinguish between direct and time-delayed escapes in the case of DI. For instance, calculating the flux through A–D border allows us to obtain ionisation yield for the direct double ionisation (direct DI), whereas calculations of the flux through S–D border will give the ionisation yield for the time-delayed emissions. Note, however, that due to this procedure a few distinct physical mechanisms are covered by this process (see the detailed discussion in the next section). In the case of TI the situation is much worse as different scenarios are possible: the electrons may ionise one by one ($0 \to 1 \to 2 \to 3$), all three electrons may ionise at once ($0 \to 3$), direct DI may be followed by a single electron emission ($0 \to 2 \to 3$) or the latter processes may occur in reversed order ($0 \to 1 \to 3$). The process of simultaneous escape of all three electrons ($0 \to 3$) we will call the direct triple ionisation (direct TI). It is characterized by the escape through A–T border. Other scenarios involve at least two stages. The flux through S–T border may be associated in a unique way with single electron ionisation followed by direct DI ($0 \to 1 \to 3$). On the other hand the flux through D–T border informs us that a final emission corresponds to the ejection of a single electron. The value of this flux does not allow us, at this stage however, to distinguish whether that DI being the first step of the TI is a time-delayed or a direct event. We discuss this issue and its solution later in the text.

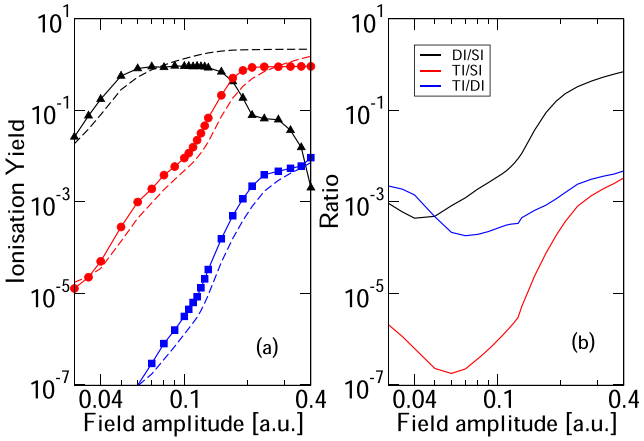

Figure 2. Panel (a): numerical ionisation yields as a function of the peak electric field amplitude in atomic units. $F_0 = 0.1$ a.u. corresponds to 5.14×10^{10} V m^{-1} or laser intensity $I = 3.5 \times 10^{14}$ W cm^{-2}. The yields are calculated at the end of a $n_c = 5$ cycle pulse. Numerical yields are shown by lines with symbols: SI (black triangles), DI (red circles) and TI (blue squares). The dashed lines with corresponding colours represent the data averaged over a Gaussian laser beam intensity distribution (see text). Panel (b): ratios of volume averaged numerical ionisation yields as a function of peak electric field amplitude in atomic units. Note that DI/SI and TI/DI do not vary significantly for small and intermediate fields.

3. Results and discussion

Let us first consider total ionisation yields as a function of the peak electric field amplitude, see figure 2(a). Results presented are obtained for the carrier–envelope phase $\varphi = 0$. Single ionisation (SI, black triangles) signal quickly saturates, then drops down for amplitudes larger than $F_0 = 0.1$ a.u.. The observed drop of SI signal is a consequence of lack of averaging over intensity profile of the pulse which is inevitable in the experiments. Assuming a Gaussian profile of the laser beam the averaged ionisation yield may be obtained as [56]:

$$P_{\mathrm{avg}}(I_0) \propto \int_0^{I_0} \frac{P(I)}{I}\,\mathrm{d}I. \tag{7}$$

The averaged SI yield is depicted with dashed black line in figure 2(a). As expected, once the saturation level is achieved

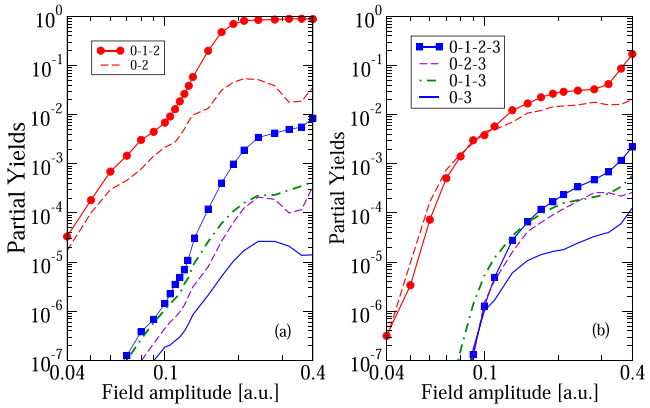

Figure 3. Different partial yields corresponding to different paths leading to DI and TI events. Panel (a) shows the data corresponding to yields for p^3 initial configuration, panel (b) to s^2p^1 initial state. Common legends for both panels indicate that red lines with circles correspond to time-delayed DI, red dashed lines to direct DI. For TI blue line with squares corresponds to a time-delayed triple escape $0 \to 1 \to 2 \to 3$. Dashed violet line presents direct DI followed by SI and dash-dotted green line shows SI followed by direct DI. Solid blue line with no symbols represent a direct TI.

it does not drop, because the higher the intensity the lower the weight given to the respective yield. The same averaging procedure is used for DI and TI yields and is indicated by the corresponding dashed lines. Analysing both the full DI yield (red circles) and its averaged counterpart (dashed red line) in figure 2(a) one may see the weak trace of the characteristic knee for amplitudes close to $F_0 = 0.1$ a.u.. For larger field amplitude values DI signal still grows and then saturates eventually. Similar behaviour is observed for TI yields, both non-averaged (blue squares) and averaged (dashed blue line).

Figure 2(b) shows the volume average yields in a slightly different way, not their absolute value but rather their ratios. This approach seems more reliable as our reduced dimensionality model with all attempts to reproduce the realistic ionisation yield cannot be expected to give quantitative predictions about the physics in the full space. Rather it shows trends and qualitative features. Furthermore, the minima of the ratios give us analogous, but somewhat more precise information about the onset of the knees visible in the absolute ionisation yields. It is quite reassuring to observe that the ratio of DI to SI yields (black line in figure 2(b)) is practically constant for field amplitude values corresponding to the characteristic knee in the yield curve and is of the order of 10^{-3} as reported in experiments [5, 24]. The ratio of triple to SI yields (red line in figure 2(b)) shows a bigger variation with F_0.

Importantly, multi-ionisation signals may be further separated into different components due to the applied method of calculating yields as summarized in figure 3(a). First, the DI signal is divided into two contributions, i.e. direct DI (dashed red line) and the time-delayed process (red circles). Recall that direct DI is found by counting the flux through A–D. The time-delayed process appears as a sequential DI as it is given by the flux through S–D border. It is, however, a combination of different physical processes that cannot be, unfortunately, separated further in our approach. Former studies of two electron processes identified different ionisation channels. Direct DI is sometimes called a recollision impact ionisation, also known as an electron impact ionisation or a recollision induced direct ionisation [57–59]. The time-delayed processes, in which one electron leaves the atom after some delay with respect to the first one, may be again divided into genuine sequential DI and recollision excitation with a subsequent ionisation (RESI) [7, 60, 61]; yet another time-delayed mechanism proposed recently is 'slingshot non-sequential DI' [62]. The time-delayed double ionisation (time-delayed DI) thus contains also RESI yields despite RESI being physically a non-sequential process. This is a significant drawback of our approach affecting the interpretation of the results. In particular, the knee feature of the ionisation yield curve is commonly considered as a manifestation of RESI. Yet we have no observable to distinguish between RESI and the truly sequential process. For that reason the characteristic knee appears in DI signal for time-delayed DI component, figure 3(a). Time-delayed DI signal rapidly grows for field amplitudes larger than $F_0 = 0.1$, while direct DI yield saturates at the level which is two orders of magnitude lower. Such a behaviour is expected for strong fields for which sequential ionisation prevails over other processes.

Figure 3(b) shows the corresponding data obtained for s^2p^1 initial configuration for comparison (with data partially reported in [38], here supplemented by additional points). Comparing both panels one easily notices that the two-electron knee is much more pronounced for s^2p^1 initial configuration. This is understandable as for p^3 configuration the antisymmetric character of the wavefunction prohibits close encounter and strong rescattering thus RESI processes are expected to be much less efficient than for s^2p^1 case. Additionally, as noted for p^3 configuration direct DI saturates at the level which is two orders of magnitude lower than the time-delayed DI signal, whereas for s^2p^1 configuration both channels give comparable yields and only at high field amplitudes ($F > 0.3$) the time-delayed DI signal starts to grow rapidly. That difference is again a consequence of the antisymmetric character of the wavefunction for p^3 and closely resembles reported suppression of NSDI for the ^3S metastable state in He [63].

It is interesting to look at different TI contributions. The method of calculating ionisation yields allows to straightforwardly differentiate TI signal into three different contributions, namely, direct escape (flux through A–T border in figure 1(b)), and two mixed paths, i.e. SI followed by direct DI (flux through S–T border) and DI followed by SI (flux through D–T border), where DI means any kind of DI, that is direct or time-delayed. Therefore, the latter of these two mixed paths comprise some portion of process that is fully sequential.

To resolve the above described ambiguity we use an approach proposed by us while analysing the case of s^2p^1 electron configuration [36], namely, we estimate different contributions to TI based on what we learned from DI in the same set-up. More precisely, we assume that the ratio of time-delayed to direct DI, as determined by the fluxes through S–D and A–D, holds for DI being the intermediate step in the three-electron process. Such an assumption allows us to extract the time-delayed contribution from the mixed path calculated with use of the flux through D–T border. The results are presented

in figure 3(a). The signal that corresponds to a direct escape of three electrons ($0 \to 3$) is marked with the solid blue line, signals corresponding to partially direct escapes are marked with dashed violet and dash-dotted green lines, and finally, signal for the time-delayed triple escape is marked with blue squares. As expected the time-delayed TI ($0 \to 1 \to 2 \to 3$) dominates over the whole range of field amplitudes, the other channels give non-negligible but much weaker contributions. The two partially direct escapes, i.e. a direct DI followed by a SI ($0 \to 2 \to 3$) and SI is followed by a direct DI ($0 \to 1 \to 3$) both give comparable yields which saturate at the level of two orders of magnitude lower than the time-delayed TI. The weakest of all is the direct TI yield ($0 \to 3$). The observed hierarchy of contributions is different from that obtained for Li-like atoms as reported earlier [36, 38] for which direct escape was the least important channel of ionisation and the other three channels gave comparable contributions. For a direct comparison those events are shown in figure 3(b). We attribute the observed hierarchy of contributions mainly to the antisymmetry of the initial wavefunction for p^3—due to the Pauli principle: the equivalent electrons cannot come too close to each other and thus the rescattering, important for non-sequential ionisation, is reduced.

For both p^3 and s^2p^1 initial configurations data shown in figure 3 are extracted after the end of the five-cycle pulse. Also the splitting of the configuration space into different regions (as defined by r_a, r_b, r_c—see section 2.2) is assumed the same in both cases making the comparison of physics in both cases possible.

It may be difficult if not impossible to distinguish between different processes via measurement of yields alone. However, one may expect that a difference in the hierarchy of contribution may influence electron's momentum distribution and thus be accessible in future experiments. Similarly, suppression of NSDI for the ^3S metastable state in He was evident in both the electron and ion momentum distributions [63].

4. Conclusions

We have studied TI of atoms with p^3 valence shell. To this end we employed the restricted-geometry model with three active electrons each moving along a single line formed by saddles of the effective adiabatic potential. Such a model allows for a detailed numerical analysis on a finite size grid. By dividing the configuration space into separate regions we were able to estimate the role of different non-sequential and time-delayed ionisation processes. The obtained ionisation yields feature trends that may be observed in experiments—to facilitate it we present also the yields averaged over the Gaussian profile of the laser beam.

The laser field amplitude dependence of the ionisation yields is significantly different in the present case (p^3 valence shell) from previously considered by us s^2p^1 configuration of active electrons. For s^2p^1 initial state we observed a pronounced knee which reveals the importance of the non-sequential DI as well as the traces of the knee in three electron ionisation [36]. For direct DI we have shown that this channel is dominated by electrons with opposite spin [38]. In the present case of three equivalent electrons we have found that non-sequential two and three electron processes are strongly suppressed and the sequential ionisation dominates both the DI and the TI yields. This behaviour we associate with reduced rescattering between identically spin oriented electrons—the Pauli principle (and the corresponding antisymmetric pairwise wavefunction) does not allow the electrons to come into a close contact and exchange energy efficiently.

Our findings should have a direct significance for qualitative features of strong field ionisation of atoms with p^3 valence shell. We believe that the observed difference between ionisation yields for different electronic configuration will have also a significant manifestation in ejected electron momenta distributions. Work in that direction is in progress.

Acknowledgments

We are grateful to Artur Maksymov for the help with the computer code. This work was supported by National Science Centre, Poland via Symfonia Project No. 2016/20/W/ST4/00314 (MM, JPB and JZ). We also acknowledge the support of PL-Grid Infrastructure where all numerical calculations were carried out.

Data availability statement

All data that support the findings of this study are included within the article (and any supplementary files).

ORCID iDs

Jakub S Prauzner-Bechcicki https://orcid.org/0000-0003-3986-1898
Dmitry K Efimov https://orcid.org/0000-0002-1264-4044
Michał Mandrysz https://orcid.org/0000-0001-6059-0370
Jakub Zakrzewski https://orcid.org/0000-0003-0998-9460

References

[1] Liu W-C, Eberly J H, Haan S L and Grobe R 1999 Correlation effects in two-electron model atoms in intense laser fields *Phys. Rev. Lett.* **83** 520–3
[2] Bergues B *et al* 2012 Attosecond tracing of correlated electron-emission in non-sequential double ionization *Nat. Commun.* **3** 813
[3] Fittinghoff D N, Bolton P R, Chang B and Kulander K C 1992 Observation of nonsequential double ionization of helium with optical tunneling *Phys. Rev. Lett.* **69** 2642–5
[4] Kondo K, Sagisaka A, Tamida T, Nabekawa Y and Watanabe S 1993 Wavelength dependence of nonsequential double ionization in He *Phys. Rev.* A **48** R2531–3
[5] Walker B, Sheehy B, DiMauro L F, Agostini P, Schafer K J and Kulander K C 1994 Precision measurement of strong field double ionization of helium *Phys. Rev. Lett.* **73** 1227–30
[6] Staudte A *et al* 2007 Binary and recoil collisions in strong field double ionization of helium *Phys. Rev. Lett.* **99** 263002
[7] Rudenko A, de Jesus V L B, Ergler T, Zrost K, Feuerstein B, Schröter C D, Moshammer R and Ullrich J 2007 Correlated two-electron momentum spectra for strong-field nonsequential double ionization of He at 800 nm *Phys. Rev. Lett.* **99** 263003

[8] Corkum P B 1993 Plasma perspective on strong field multiphoton ionization *Phys. Rev. Lett.* **71** 1994–7

[9] L'Huillier A, Lompre L A, Mainfray G and Manus C 1982 Multiply charged ions formed by multiphoton absorption processes in the continuum *Phys. Rev. Lett.* **48** 1814–7

[10] l'Huillier A, Lompre L A, Mainfray G and Manus C 1983 Multiply charged ions induced by multiphoton absorption in rare gases at 0.53 μm *Phys. Rev.* A **27** 2503–12

[11] Luk T S, Pummer H, Boyer K, Shahidi M, Egger H and Rhodes C K 1983 Anomalous collision-free multiple ionization of atoms with intense picosecond ultraviolet radiation *Phys. Rev. Lett.* **51** 110–3

[12] Boyer K, Egger H, Luk T S, Pummer H and Rhodes C K 1984 Interaction of atomic and molecular systems with high-intensity ultraviolet radiation *J. Opt. Soc. Am.* B **1** 3–8

[13] Luk T S, Johann U, Egger H, Pummer H and Rhodes C K 1985 Collision-free multiple photon ionization of atoms and molecules at 193 nm *Phys. Rev.* A **32** 214–24

[14] Chin S L, Yergeau F and Lavigne P 1985 Tunnel ionisation of Xe in an ultra-intense CO_2 laser field (10^{14} W cm^{-2}) with multiple charge creation *J. Phys. B: At. Mol. Phys.* **18** L213–5

[15] Lambropoulos P 1985 Mechanisms for multiple ionization of atoms by strong pulsed lasers *Phys. Rev. Lett.* **55** 2141–4

[16] Yergeau F, Chin S L and Lavigne P 1987 Multiple ionisation of rare-gas atoms by an intense CO_2 laser (10^{14} W cm^{-2}) *J. Phys. B: At. Mol. Phys.* **20** 723–39

[17] Crance M 1987 Multiphoton stripping of atoms *Phys. Rep.* **144** 118–85

[18] Mu X-D, Åberg T, Blomberg A and Crasemann B 1986 Production of multiply charged ions by strong UV laser pulses: theoretical evidence for stepwise ionization *Phys. Rev. Lett.* **56** 1909–12

[19] Åberg T, Blomberg A, Tulkki J and Goscinski O 1984 Maximum entropy theory of recoil charge distributions in electron-capture collisions *Phys. Rev. Lett.* **52** 1207–10

[20] Geltman S 1985 Multiple ionization of a Hartree atom by intense laser pulses *Phys. Rev. Lett.* **54** 1909–12

[21] Zakrzewski J 1986 On the Geltman–Hartree model of multiple ionisation by intense laser pulses *J. Phys. B: At. Mol. Phys.* **19** L315–9

[22] Lewenstein M 1986 Collective effects at high laser intensities and multiple ionisation *J. Phys. B: At. Mol. Phys.* **19** L309–14

[23] Geltman S and Zakrzewski J 1988 Multiple ionisation by intense laser pulses in the independent-electron model: application to xenon *J. Phys. B: At. Mol. Opt. Phys.* **21** 47–62

[24] Larochelle S, Talebpour A and Chin S L 1998 Non-sequential multiple ionization of rare gas atoms in a Ti:Sapphire laser field *J. Phys. B: At. Mol. Opt. Phys.* **31** 1201

[25] Parker J S, Smyth E S and Taylor K T 1998 Intense-field multiphoton ionization of helium *J. Phys. B: At. Mol. Opt. Phys.* **31** L571

[26] Parker J S, Glass D H, Moore L R, Smyth E S, Taylor K T and Burke P G 2000 Time-dependent and time-independent methods applied to multiphoton ionization of helium *J. Phys. B: At. Mol. Opt. Phys.* **33** L239

[27] Parker J S, Doherty B J S, Taylor K T, Schultz K D, Blaga C I and DiMauro L F 2006 High-energy cutoff in the spectrum of strong-field nonsequential double ionization *Phys. Rev. Lett.* **96** 133001

[28] Feist J, Nagele S, Pazourek R, Persson E, Schneider B I, Collins L A and Burgdörfer J 2008 Nonsequential two-photon double ionization of helium *Phys. Rev.* A **77** 043420

[29] Hao X, Chen J, Li W, Wang B, Wang X and Becker W 2014 Quantum effects in double ionization of argon below the threshold intensity *Phys. Rev. Lett.* **112** 073002

[30] Lein M, Gross E K and Engel V 2000 Intense-field double ionization of helium: identifying the mechanism *Phys. Rev. Lett.* **85** 4707

[31] Ruiz C, Plaja L, Roso L and Becker A 2006 *Ab initio* calculation of the double ionization of helium in a few-cycle laser pulse beyond the one-dimensional approximation *Phys. Rev. Lett.* **96** 053001

[32] Prauzner-Bechcicki J S, Sacha K, Eckhardt B and Zakrzewski J 2008 Quantum model for double ionization of atoms in strong laser fields *Phys. Rev.* A **78** 013419

[33] Prauzner-Bechcicki J S, Sacha K, Eckhardt B and Zakrzewsk J 2007 Time-resolved quantum dynamics of double ionization in strong laser fields *Phys. Rev. Lett.* **98** 203002

[34] Eckhardt B, Prauzner-Bechcicki J S, Sacha K and Zakrzewsk J 2010 Phase effects in double ionization by strong short pulses *Chem. Phys.* **370** 168–74

[35] Chen S, Ruiz C and Becker A 2010 Double ionization of helium by intense near-infrared and VUV laser pulses *Phys. Rev.* A **82** 033426

[36] Thiede J H, Eckhardt B, Efimov D K, Prauzner-Bechcicki J S and Zakrzewski J 2018 *Ab initio* study of time-dependent dynamics in strong-field triple ionization *Phys. Rev.* A **98** 031401

[37] Efimov D K, Maksymov A, Prauzner-Bechcicki J S, Thiede J H, Eckhardt B, Chacón A, Lewenstein M and Zakrzewski J 2018 Restricted-space *ab initio* models for double ionization by strong laser pulses *Phys. Rev.* A **98** 013405

[38] Efimov D K, Prauzner-Bechcicki J S, Thiede J H, Eckhardt B and Zakrzewski J 2019 Double ionization of a three-electron atom: spin correlation effects *Phys. Rev.* A **100** 063408

[39] Mandrysz M, Kübel M, Zakrzewski J and Prauzner-Bechcicki J S 2019 Rescattering effects in streaking experiments of strong-field ionization *Phys. Rev.* A **100** 063410

[40] Efimov D K, Prauzner-Bechcicki J S and Zakrzewski J 2020 Strong-field ionization of atoms with p^3 valence shell: two versus three active electrons *Phys. Rev.* A **101** 063402

[41] Grobe R, Rzazewski K and Eberly J H 1994 Measure of electron–electron correlation in atomic physics *J. Phys. B-At. Mol. Opt.* **27** L503–8

[42] Sacha K and Eckhardt B 2001 Nonsequential triple ionization in strong fields *Phys. Rev.* A **64** 053401

[43] Emmanouilidou A and Rost J M 2006 The coulomb four-body problem in a classical framework: triple photoionization of lithium *J. Phys. B: At. Mol. Opt.* **39** 4037–48

[44] Ho P J and Eberly J H 2007 Argon-like three-electron trajectories in intense-field double and triple ionization *Opt. Express* **15** 1845–50

[45] Ho P J and Eberly J H 2006 In-plane theory of nonsequential triple ionization *Phys. Rev. Lett.* **97** 083001

[46] Zhou Y, Liao Q and Lu P 2010 Complex sub-laser-cycle electron dynamics in strong-field nonsequential triple ionization *Opt. Express* **18** 16025

[47] Tang Q, Huang C, Zhou Y and Lu P 2013 Correlated multielectron dynamics in mid-infrared laser pulse interactions with neon atoms *Opt. Express* **21** 21433

[48] Schulz M, Moshammer R, Schmitt W, Kollmus H, Mann R, Hagmann S, Olson R E and Ullrich J 2000 Correlated three-electron continuum states in triple ionization by fast heavy-ion impact *Phys. Rev.* A **61** 022703

[49] Schulz M, Moshammer R, Fischer D and Ullrich J 2004 Two-particle versus three-particle interactions in single ionization of helium by ion impact *J. Phys. B: At. Mol. Opt.* **37** 4055

[50] Rudenko A, Zrost K, Feuerstein B, de Jesus V L B, Schröter C D, Moshammer R and Ullrich J 2004 Correlated multielectron dynamics in ultrafast laser pulse interactions with atoms *Phys. Rev. Lett.* **93** 253001

[51] Rudenko A, Ergler T, Zrost K, Feuerstein B, B de Jesus V L, Schröter C D, Moshammer R and Ullrich J 2008 From nonsequential to sequential strong-field multiple ionization: identification of pure and mixed reaction channels *J. Phys. B: At. Mol. Opt. Phys.* **41** 081006

[52] Arnol'd V I 2013 *Mathematical methods of classical mechanics* vol 60 (Berlin: Springer)
[53] Eckhardt B and Sacha K 2006 Classical threshold behaviour in a (1 + 1)-dimensional model for double ionization in strong fields *J. Phys. B: At. Mol. Opt. Phys.* **39** 3865
[54] Ruiz C, Plaja L and Roso L 2005 Lithium ionization by a strong laser field *Phys. Rev. Lett.* **94** 063002
[55] Dundas D, Taylor K T, Parker J S and Smyth E S 1999 *J. Phys. B: At. Mol. Opt.* **32** L231
[56] Strohaber J, Kolomenskii A A and Schuessler H A 2015 Highly ionized xenon and volumetric weighting in restricted focal geometries *J. Appl. Phys.* **118** 083107
[57] Weber T *et al* 2000 *Phys. Rev. Lett.* **84** 443
[58] Weber T *et al* 2000 Correlated electron emission in multiphoton double ionization *Nature* **405** 658
[59] Moshammer R *et al* 2000 *Phys. Rev. Lett.* **84** 447
[60] Figueira de Morisson Faria C and Liu X 2011 Electron–electron correlation in strong laser fields *J. Mod. Opt.* **58** 1076–131
[61] ShaaranT andFigueira de Morisson Faria C 2010 Laser-induced nonsequential double ionization: kinematic constraints for the recollision-excitation-tunneling mechanism *J. Mod. Opt.* **57** 984–91
[62] Katsoulis G P, Hadjipittas A, Bergues B, Kling M F and Emmanouilidou A 2018 Slingshot nonsequential double ionization as a gate to anticorrelated two-electron escape *Phys. Rev. Lett.* **121** 263203
[63] Eckhardt B, Prauzner-Bechcicki J S, Sacha K and Zakrzewski J 2008 Suppression of correlated electron escape in double ionization in strong laser fields *Phys. Rev.* A **77** 015402